Institute of Experimental Morphology, Pathology and Anthropology with Museum
Bulgarian Anatomical Society

Acta Morphologica et Anthropologica, 32 (3-4)
Sofia ● 2025

Accelerated Aging Model Effects in the Colorectal Region

Nikolay Genov[1], Nikolay Dimitrov[1], Lubomir Petrov[2,3], Elina Tsvetanova[3], Albena Alexandrova[2,3], Dimitrinka Atanasova[1,3*]*

[1] Department of Anatomy, Faculty of Medicine, Trakia University, Stara Zagora, Bulgaria
[2] National Sports Academy "Vassil Levski", Sofia, Bulgaria
[3] Institute of Neurobiology, Bulgarian Academy of Sciences, Sofia, Bulgaria

* Corresponding authors e-mails: nikolay.genov@trakia-uni.bg
dimitrinka.atanasova-dimitrova@trakia-uni.bg

D-galactose is widely used to induce accelerated aging, oxidative stress, neurodegeneration, and inflammation, but its effects on the large intestine remain poorly understood. We studied male ICR mice divided into two groups: a control group and a group treated with D-galactose (500 mg/kg/day, orally, for 6 weeks). Histological slides were obtained from all levels of the large intestine and were stained with Azan, van Gieson and Toluidine blue. Azan staining demonstrated an increase in collagen fibers in the proximal colon by over 30% and in the rectum by 73% in D-galactose-treated mice compared to the control group. Van Gieson staining showed 83% increase in the periganglionic space in the proximal colon compared to the control group. Toluidine blue staining for mast cells demonstrated an increase of over 30% in the proximal colon, a 48% increase in the rectum, and a nine-fold higher density of mast cells in the distal colon.

Key words: D-galactose–induced aging, ICR mice, large intestine, myenteric plexus, periganglionic space, collagen deposition

Introduction

The gastrointestinal tract possesses an intrinsic neural network—comprising neurons, glial cells, and ganglia organised into the myenteric (Auerbach's) and submucosal (Meissner's) plexuses – collectively referred to as the enteric nervous system (ENS) [5, 6]. The ganglia of the Auerbach plexus are encapsulated by a structure composed of extracellular matrix (ECM) molecules such as agrin and collagen type 4 (Col4), playing a role as a blood-myenteric barrier (BMB) [4]. It is reported that the amount of collagen deposition (predominantly collagen type I) around the ganglia increases with age [10, 7]. Enteric neuroinflammation induced by various reasons could cause neurodegeneration and disruption of the capsule providing BMB [6, 4]. Neuronal loss

in the myenteric plexus is commonly reported as a change occurring with advanced aging [15]. The use of D-galactose is known as the safest method to induce accelerated aging-related changes in vivo by increasing reactive oxygen species (ROS) as well as inflammatory cytokine levels [1]. At the colonic level, it causes a significant reduction in neuron cell bodies [8]. D-galactose has been shown to disrupt the structure of the intestinal mucosa, thereby compromising the intestinal barrier [17].

No studies have focused on the changes that this accelerated ageing model has on the BMB and the components of the ECM around the myenteric plexus. The present research aimed to demonstrate the shifts induced by our model around the ganglia of the Auerbach plexus and the inflammatory response it triggers at different levels of the *intestinum crassum*.

Material and Methods

For this experiment, twelve (n=12) sexually mature male ICR mice (body mass 25–30g) were brought in from the Breeding facility for Laboratory Animals, Slivnitsa, Bulgaria. The animals were acclimated for 7 days before the experiment and then randomly allocated to a control group (K1, n = 6) or a D-galactose-treated group (D-gal, n = 6). The mice were kept under standard laboratory conditions, which consisted of a 12:12 h light–dark cycle, and they were given free access to food and water. Their housing conditions were: temperature (21–23°C), relative humidity (45–65%) and cage type (Type II polysulfone).

D-galactose was administered ad libitum in the drinking water for 6 weeks at an average daily dose of 500 mg/kg. All procedures were approved by the Bulgarian Food Safety Agency and complied with Directive 2010/63/EU on the protection of animals used for scientific purposes (approval No. 424/24.02.2025).

To perform the morphometric analysis, all animals were anaesthetised with 87 mg ketamine/kg body weight combined with 13 mg xylazine/kg, administered by simultaneous intraperitoneal injections. The intestinum crassum of the examined animals was dissected, cleared under running water, and submerged in 4% paraformaldehyde overnight at a temperature of 4°C. Samples were then divided into proximal colon (PC), distal colon (DC) and rectum (REC). The standard protocol for embedding tissue samples in paraffin was applied. 6 µm sections were taken from the paraffin blocks and mounted onto chrome gelatinised glass slides. Standard protocols for Azan, van Gieson and Toluidine blue staining were applied.

The following morphological characteristics were evaluated: percentage of collagen fibers in the preganglionic space as part of the area of the entire ganglion (C%), as well as mast cell density in the samples (MCd). MCd was presented as a mast cell count per mm^2 (mc/mm^2).

Each of the glass slides was carefully examined under the research microscope, Leica DM1000, equipped with a digital camera, Leica DFC 290. Adobe Photoshop 24.1.0 was used to enhance the contrast and provide a more precise representation of the studied structures.

For the morphometric analysis, the graphic software ImageJ (National Institutes of Health, Bethesda, MD, USA) was employed. The plug-in ColourDeconvolution2

helped us measure the percentage of the connective tissue surrounding the ganglia of the ENS by separating the different colors of the used stain.

The statistical data were analysed using GraphPad Prism 8 software (San Diego, CA, USA). We used: Shapiro-Wilk test for normal distribution of the studied values, as well as Dunn's multiple comparisons test, or Ordinary one-way ANOVA (depending on the distribution of the values) to determine the significance of the collected data. Statistical significance was determined if p-values were <0.05.

Results

Collagen fibers surrounding the myenteric ganglia were visualised with classical histochemical stains – Azan trichrome (**Fig. 1C-D**) and van Gieson (**Fig. 1A-B**). Azan delineated collagen as a well-defined blue–green meshwork adjacent to the *plexus myentericus*. Tangential and transverse sections, 6 µm thick, were examined. The proportion of collagenous connective tissue relative to total ganglionic area (C%) was quantified across n = 69 ganglia. Because the data were non-normally distributed, results are reported as medians and group differences were assessed using a Kruskal –

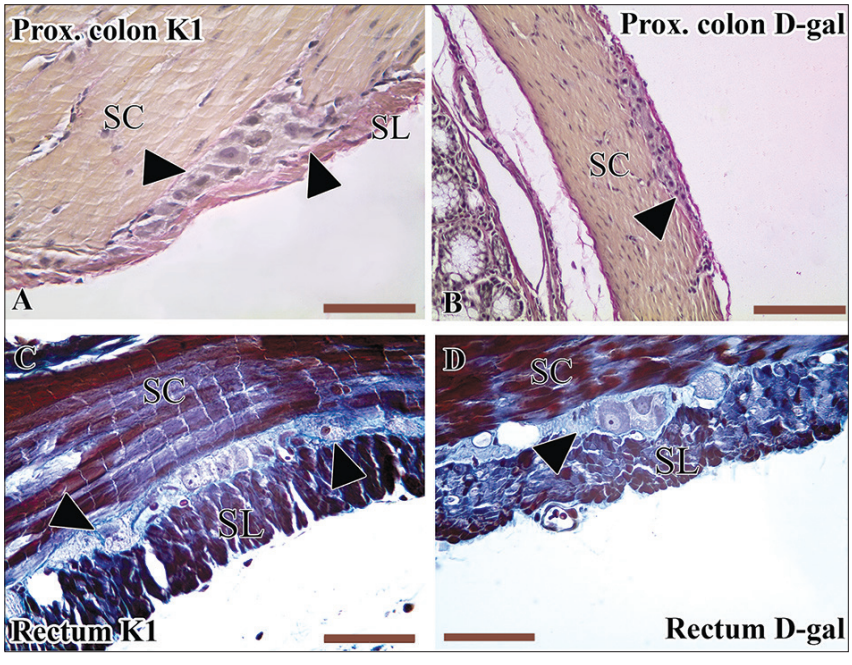

Fig. 1. Van Gieson (A-B) and Azan (C-D) staining of transverse cut of proximal colon (A) and sagittal cut of proximal colon (B) and rectum (C-D) of the control group K1 (A, C) and D-Galactose treated one (B, D) in ICR mice. Arrowheads indicate the collagen fibres around the preganglionic space. SL-stratum longitudinale, SC – stratum circulare. Scale bars = 50 µm (A, C, D), 100 µm (B).

Wallis test followed by Dunn's multiple comparisons. Overall differences in C% were observed ($H(5) = 23.07$, $p = 0.0003$). Median (Mdn) values were: PC–K1 = 12.22, D-Gal = 16.84; DC–K1 = 18.53, D-Gal = 11.67; REC–K1 = 9.344, D-Gal = 16.18 (**Fig. 3B**). Relative to controls, D-galactose exposure produced a marked reduction in C% at the DC level (by almost 60% decrease; $p = 0.0063$) and a significant increase at the REC level (73% increase; $p = 0.0075$) (**Fig. 3A**).

Using van Gieson staining (**Fig. 1A-B**), collagen surrounding myenteric ganglia appeared with the characteristic red coloration. A total of 79 ganglia were analyzed across control (K1) and D-galactose–treated (D-Gal) groups. Because C% (collagen area as a percentage of total ganglionic area) was not normally distributed, group differences were evaluated with the Kruskal – Wallis test, which indicated a significant overall effect ($H(5) = 22.52$, $p = 0.0004$) (**Fig. 3B**). Dunn's post hoc analysis showed a significant increase in C% in the proximal colon, with medians rising from 8.056 (K1) to 14.78 (D-Gal; $p < 0.05$). In the distal colon, C% likewise increased by 47% relative to controls (control median = 6.3; $p < 0.05$) (**Fig. 3B**).

Mast cells were visualized using toluidine blue staining (**Fig. 2A-B**). Mast cell (MC) density was expressed as cells per mm². Mast cell (MC) density was expressed as cells per mm² (**Fig. 3C-D**). In total, 36 histological slides were examined (K1, n = 18; D-Gal, n = 18), with 183 MCs identified. Normality was assessed with the Shapiro–Wilk test; data are reported as mean ± SD. One-way ANOVA across the six groups showed a significant overall effect, $F(5,30) = 12.69$, $p < 0.0001$. In controls (K1), MC density was highest in the rectum (REC: 1.041 ± 0.6584 cells/mm²) and proximal colon (PC: 0.7528 ± 0.2320 cells/mm²), and lowest in the distal colon (DC: 0.3259 ± 0.2035 cells/mm²) (**Fig. 3D**). Following D-galactose exposure, MC density increased and redistributed across segments, peaking in the DC (2.907 ± 1.172 cells/mm²), followed by the REC (1.541 ± 0.3905 cells/mm²) and PC (0.9948 ± 0.4704 cells/mm²) (**Fig. 3C**).

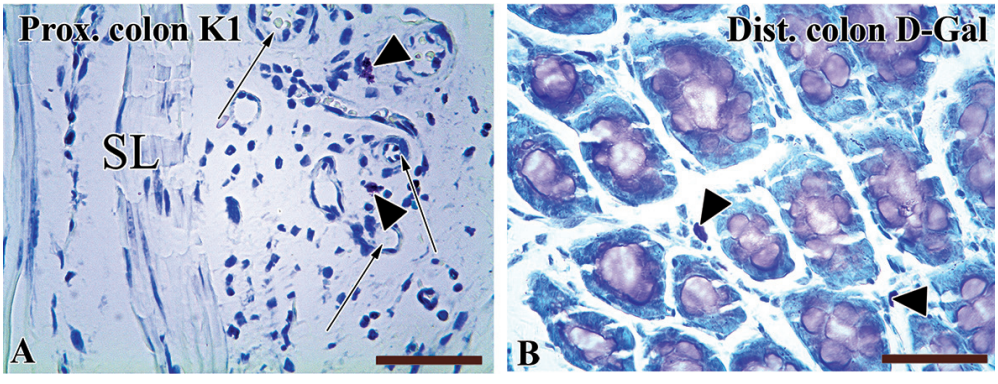

Fig. 2. Microphotographs stained with Toluidine blue of the proximal colon in the control group (A) and the distal colon in D-galactose-treated mice (B). Arrowheads are pointing at mast cells situated between the stratum longitudinale (A) and the mucosa (B). Arrows indicate small blood vessels; SL-stratum longitudinale. Scale bars = 50 μm.

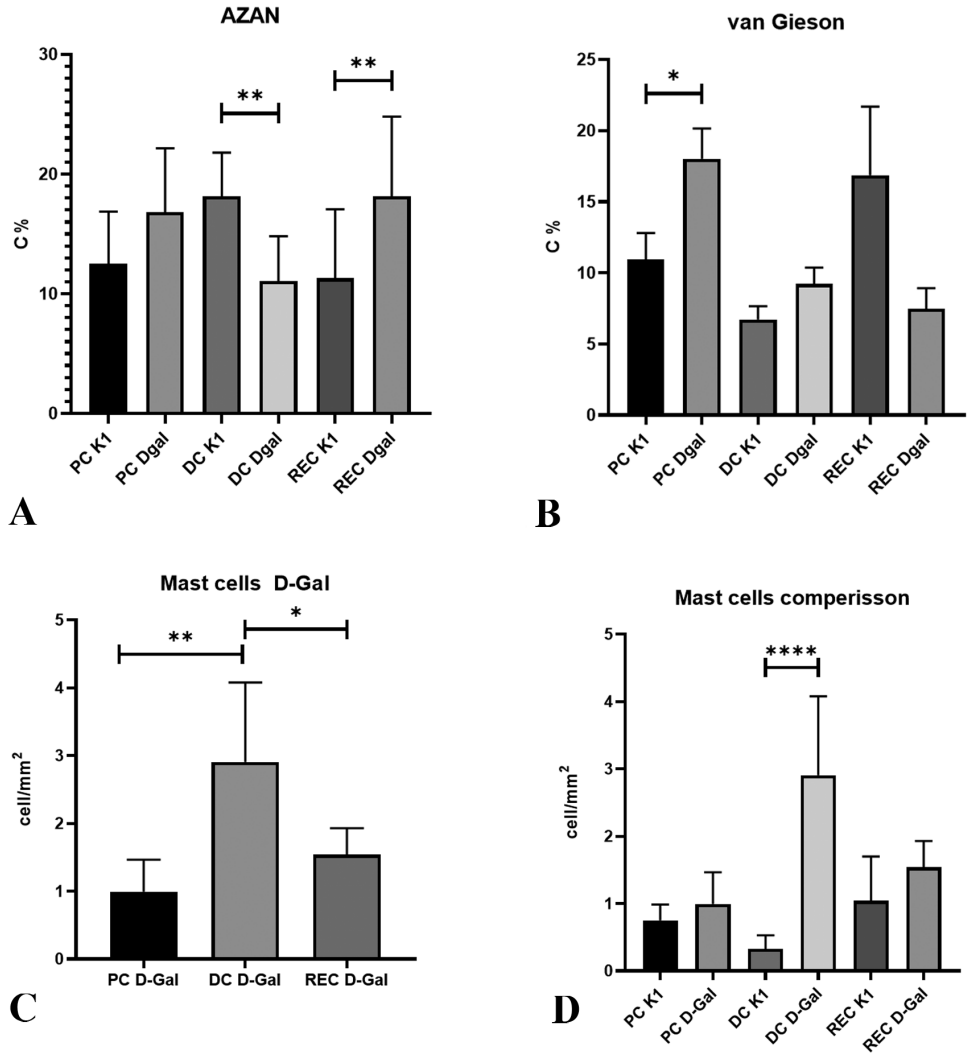

Fig. 3. Histograms showing (A–B) the percentage area of collagen fibers relative to the area of myenteric ganglia in Azan (A) and Van Gieson (B)–stained sections, and (C–D) the distribution of mast cells across different segments of the large intestine in K1 (control) and D-galactose–treated mice. Error bars indicate SD. Data were compared using the Kruskal–Wallis test followed by Sidak's multiple comparisons test; *$p < 0.05$, **$p < 0.01$, ****$p < 0.0001$.

Discussion

Our study extends previous work on the D-galactose–accelerated aging model by shifting the focus from the well-described neurodegeneration of the myenteric plexus [8] to remodeling of the myenteric ganglionic capsule and associated inflammatory responses across levels of the large intestine in ICR mice. Consistent with prior reports,

gastrointestinal aging is accompanied by an increase in collagen deposition [2]. The collagen family includes more than 20 subtypes, commonly grouped into fibril-forming (types I–III) and network-forming (type IV) categories [16], with type IV as the predominant collagen of the ganglionic basement membrane in the myenteric plexus [4].

Our approach integrates complementary histological stains with attention to their interpretive limits. Van Gieson staining, widely used to visualise type I collagen [11] and in our previous work [7], serves as a practical indicator of fibrillar collagen within and around myenteric ganglia. In contrast, Azan staining is a non-specific method for demonstrating collagen [9]; its findings require follow-up immunohistochemical analyses to resolve collagen subtype composition and provide detailed characterisation. Our analysis centres on capsule remodeling and inflammation as key features of D-galactose–induced aging in the enteric environment, while acknowledging the need for immunohistochemical confirmation to refine collagen profiling.

Mast cells play a key role in inflammatory processes [3]. While normally present throughout the gastrointestinal tract, increased mucosal counts indicate inflammation and are associated with conditions such as irritable bowel syndrome (IBS) [12]. In this study, we used toluidine blue staining to identify and quantify mast cells as a measure of inflammation in the large intestine. This established metachromatic dye has been used to visualize mast cells by targeting their heparin-rich granules since the late 19th century [14,13].

We observed increased mast cell concentrations at all three levels of the large intestine. Within the D-galactose model, these results align with oxidative stress and suggest that this approach can induce mast cell changes similar to those seen in IBS.

Our data indicate that D-galactose provokes remodeling of the myenteric (Auerbach's) plexus, manifested as an overall thickening of the collagenous capsule that envelops the ganglia. These findings accord with our previous observations of connective-tissue alterations around the myenteric plexus in naturally aged specimens and are consistent with reports of collagen remodeling in the ageing gut.

A region-specific divergence was observed in the distal colon. Although type I collagen increased by 47%, overall collagen fibres decreased according to the Azan stain. This suggests qualitative matrix remodeling, with a shift toward fibrillar type I collagen and a reduction in other Azan-positive components. These findings underscore the limitations of relying on single-stain assessments to infer collagen composition.

At the same intestinal level, this matrix profile was accompanied by a ninefold increase in mast cells in D-galactose–treated animals, suggesting that inflammation promotes collagen turnover and capsule restructuring. D-galactose-induced inflammation may involve mechanisms of myenteric barrier disruption similar to those seen in dextran sulfate sodium–induced colitis [4]. At the same level of the large intestine, this matrix profile coincided with a ninefold increase in mast cells in D-galactose–treated animals, suggesting that inflammation drives collagen turnover and capsule restructuring. The D-galactose-triggered inflammation may converge on mechanisms of myenteric barrier disruption similar to those described in dextran sulfate sodium–induced colitis [4].

To resolve these patterns mechanistically, additional immunolabeling for collagen subtypes and related extracellular-matrix markers, along with ultrastructural imaging, will be needed. These analyses should clarify how D-galactose–induced changes

inform the trajectory of myenteric ageing and the shifts that inflammatory diseases impose on the enteric nervous system.

Conclusions

This study is among the few to examine how an accelerated-ageing paradigm, specifically D-galactose, affects the myenteric plexus. D-galactose induced remodelling of the collagenous capsule surrounding myenteric ganglia – changes consistent with ageing – while simultaneously eliciting inflammatory responses, including marked mast cell accumulation, reminiscent of colitis and irritable bowel syndrome. The pattern was segment-specific, indicating that the colorectal region does not respond uniformly to the treatment. These findings support the use of D-galactose as a practical model for investigating the interplay between ageing, extracellular matrix organisation, and inflammation in the enteric nervous system, warranting confirmation through collagen subtyping, immunophenotyping, and functional readouts.

Acknowledgements: This research is supported by the Bulgarian Ministry of Education and Science under the "National Program Young Scientists and Postdoctoral Students – 2"; by the Bulgarian National Science Fund (contract No. КП-06-Н81/2); by the National Recovery and Resilience Plan (Project BG-RRP-2.004-0006-C02); and by the Faculty of Medicine, Trakia University – Stara Zagora (Grant No. 8/2023).

References

1. Azman, K. F., R. Zakaria. D-Galactose-induced accelerated aging model: an overview. – *Biogerontology*, **20**(6), 2019, 763-782. https://doi.org/10.1007/s10522-019-09837-y.

2. Baidoo, N., E. Crawley, C. H. Knowles, G. J. Sanger, A. Belai. Total collagen content and distribution is increased in human colon during advancing age. – *PloS One*, **17**(6), 2022, e0269689. https://doi.org/10.1371/journal.pone.0269689.

3. Collington, S. J., T. J. Williams, C. L. Weller. Mechanisms underlying the localisation of mast cells in tissues. – *Trends Immunol.,* **32**(10), 2011, 478-485. https://doi.org/10.1016/j.it.2011.08.002.

4. Dora, D., S. Ferenczi, R. Stavely, V. E. Toth, Z. V. Varga, et al. Evidence of a myenteric plexus barrier and its macrophage-dependent degradation during murine colitis: Implications in enteric neuroinflammation. – *Cell. Mol. Gastroenterol. Hepatol.*, **12**(5), 2021, 1617–1641. https://doi.org/10.1016/j.jcmgh.2021.07.003.

5. Furness, J. B. The enteric nervous system and neurogastroenterology. – *Nat. Rev. Gastroenterol. Hepatol.,* **9**(5), 2012, 286-294.

6. Furness, J. B., T. V. Nguyen, K. Nurgali, Y. Shimizu. The enteric nervous system and its extrinsic connections. – *Textbook of Gastroenterology*, 2008, 15-39. https://doi.org/10.1002/9781444303254.ch2.

7. Genov, N., N. Dimitrov, D. Atanasova. Aging of the myenteric plexus in the rat colorectal region. – *Acta Morphol. Anthropol.*, **32**(1–2), 2025, 31-36. https://doi.org/10.7546/ama.32.1-2.2025.04

8. Genov, N., N. Tomov, N. Dimitrov, T. Kirov, L. Petrov, et al. Morphometric changes of the myenteric plexus in the colon of the mice-D-galactose ageing model. – *C. R. Acad. Bulg. Sci.*, **77**(4), 2024, 576–583. https://doi.org/10.7546/CRABS.2024.04.13

9. Golberg, M., J. Kobos, E. Clarke, A. Bajaka, A. Smędra, et al. Application of histochemical stains in anatomical research: A brief overview of the methods. – *Transl. Res. Anat.*, **35**, 2024, 100294. https://doi.org/10.1016/j.tria.2024.100294.

10. Gomes, O. A., R. R. de Souza, E. A. Liberti. A preliminary investigation of the effects of aging on the nerve cell number in the myenteric ganglia of the human colon. – *Gerontology*, **43**(4), 1997, 210-217. https://doi.org/10.1159/000213852.

11. Guo, S. B., Z. J. Duan, Q. M. Wang, Q. Zhou, Q. Li, X. Y. Sun. Endogenous carbon monoxide downregulates hepatic cystathionine-γ-lyase in rats with liver cirrhosis. – *Exp. Ther. Med.*, **10**(6), 2015, 2039-2046. https://doi.org/10.3892/etm.2015.2823.

12. Panarelli, N. C., J. L. Hornick, R. K. Yantiss. What is the value of counting mast cells in gastrointestinal mucosal biopsies? – *Mod. Pathol*., **36**(2), 2023, 100005. https://doi.org/10.1016/j.modpat.2022.100005.

13. Puebla-Osorio, N., S. N. E. Sarchio, S. E. Ullrich, S. N. Byrne. Detection of Infiltrating Mast Cells Using a Modified Toluidine Blue Staining. – *Methods Mol. Biol.*, **1627**, 2017, 213-222. https://doi.org/10.1007/978-1-4939-7113-8_14

14. Ribatti, D. The staining of mast cells: A historical overview. – *Int. Arch. Allergy Immunol*., **176**(1), 2018, 55-60. https://doi.org/10.1159/000487538

15. Sri Paran, T., U. Rolle, P. Puri. Age-related changes in the myenteric plexus of the porcine bowel. – *J. Pediatr. Surg.*, **44**(9), 2009, 1771-1777. https://doi.org/10.1016/j.jpedsurg.2008.12.018

16. Tvaroška, I. Glycosylation Modulates the Structure and Functions of Collagen: A Review. – *Molecules*, **29**(7), 2024, 1417. https://doi.org/10.3390/molecules29071417

17. Zhao, Y., Z. Zeng, W. Zheng, Zhang, Z., Zhang, H. et al. Cow placenta peptides ameliorate D-Galactose-induced Intestinal Barrier Damage by Regulating TLR/NF-κB Pathway. – Vet. Sciences, **12**(3), 2025, 229. https://doi.org/10.3390/vetsci12030229